

## SUPPLEMENTARY MATERIAL

### *A 1,000-yr-old tsunami in the Indian Ocean points to greater risk for East Africa*

#### Authors

Vittorio Maselli<sup>1</sup>, Davide Oppo<sup>2</sup>, Andrew L. Moore<sup>3</sup>, Aditya Riadi Gusman<sup>4</sup>, Cassy Mtelela<sup>5</sup>, David Iacopini<sup>6</sup>, Marco Taviani<sup>7,8,9</sup>, Elinaza Mjema<sup>10</sup>, Ernest Mulaya<sup>5</sup>, Melody Che<sup>3</sup>, Ai Lena Tomioka<sup>3</sup>, Elisante Mshiu<sup>5</sup>, Joseph D. Ortiz<sup>11</sup>

#### Affiliations

<sup>1</sup> Department of Earth and Environmental Sciences, Life Sciences Centre, Dalhousie University, Halifax, Nova Scotia B3H 4R2, Canada.

<sup>2</sup> School of Geosciences, University of Louisiana at Lafayette, Lafayette, Louisiana 70504, USA

<sup>3</sup> Department of Geology, Earlham College, Richmond, Indiana 47374, USA

<sup>4</sup> GNS Science, Lower Hutt 5010, New Zealand

<sup>5</sup> Department of Geology, University of Dar es Salaam, Dar es Salaam, Tanzania

<sup>6</sup> Dipartimento di Scienze della Terra, dell'Ambiente e delle Risorse (DISTAR), Università degli Studi di Napoli Federico II, Naples 80138, Italy

<sup>7</sup> Institute of Marine Sciences, ISMAR-CNR, Bologna 40129, Italy

<sup>8</sup> Stazione Zoologica Anton Dohrn, Villa Comunale, Naples 80121, Italy

<sup>9</sup> Biology Department, Woods Hole Oceanographic Institution, Woods Hole, Massachusetts 02543, USA

<sup>10</sup> Department of Archaeology, University of Dar es Salaam, Dar es Salaam, Tanzania

<sup>11</sup> Department of Geology, Kent State University, Kent, Ohio 44242, USA

#### Section S1. Study area

The study area is located on the southern bank of Pangani Bay (Tanzania), a narrow strip of estuarine and mangrove-swamp deposits (ca. 400 meters wide) accumulating at the toe of the Bweni Escarpment (Fig. S1). The study area is north of the formation region of tropical cyclones of the southwestern Indian Ocean, as highlighted by the data on hurricane tracks provided by NOAA for the period 1848 -2019 (Fig. S1). The northern bank of the river is occupied by the modern town of Pangani. In 2016-2017, the Institute of Marine Science of the University of Dar es Salaam excavated seven large ponds (ca. 20 x 27 meters wide, and a few meters deep) to host marine fishes for research. The material extracted to create the ponds was accumulated laterally, creating a series of ridges bordering the ponds. In the manuscript we called this material Facies 4, Anthrosol. The ponds were had not yet been filled at the time when the field work for this study was performed, enabling us to dig 29 pits and two trenches up to ~1-meter deep in undisturbed sediment along their flanks. Because the excavation of the ponds removed the shallow sedimentary cover, we were able to reach Facies 3 (Tsunami deposit) with minimal digging. All field and lab work for this study was conducted under permit from the Department of Archeology, University of Dar es Salaam, and the Institute of Marine Science, and under the supervision of government officials from the Pangani District (see also the Ethics Statement).

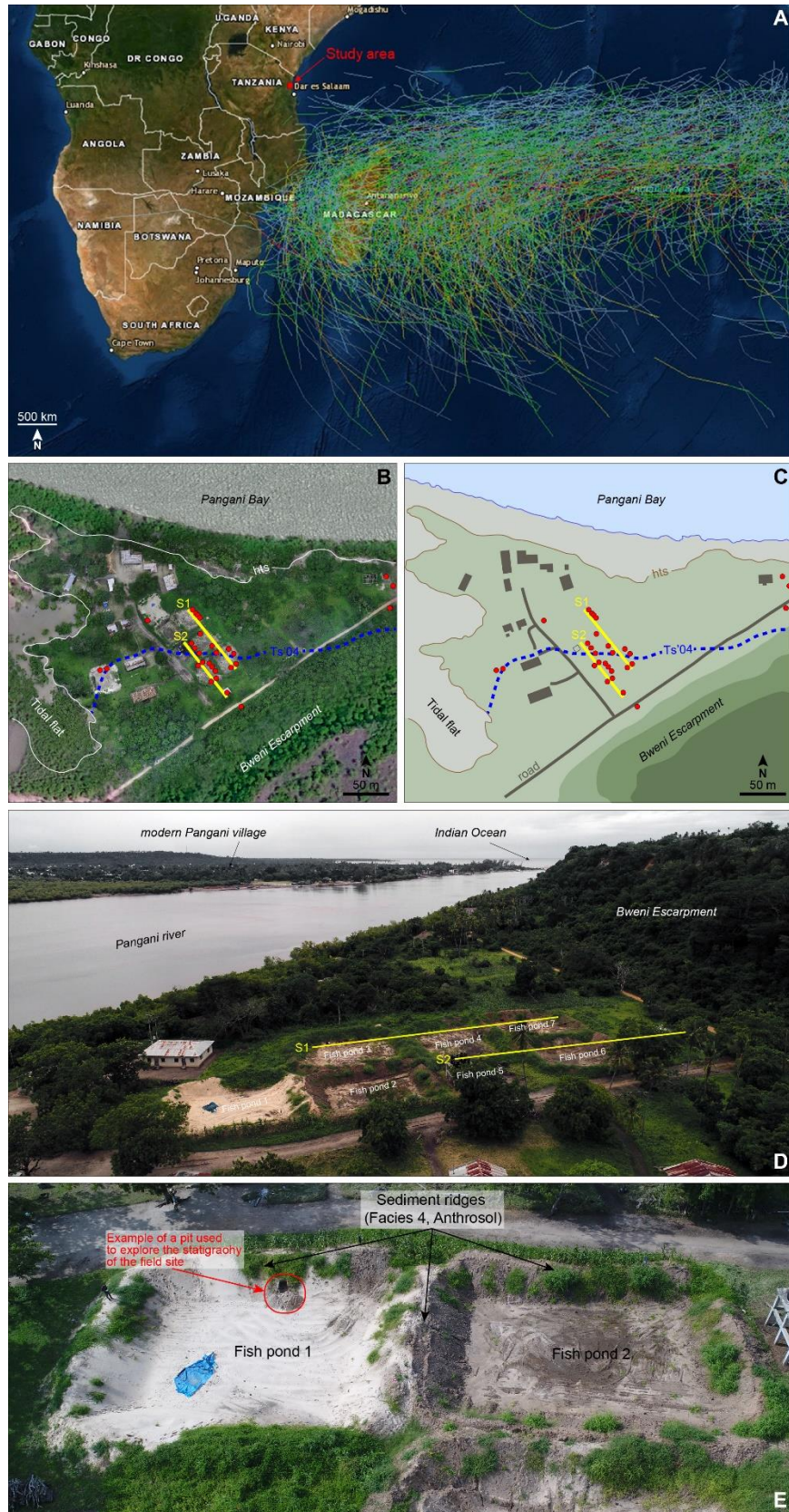


Figure S1. A: Hurricane tracks in the period 1848-2019 (source: <https://coast.noaa.gov/hurricanes>). B: aerial image of the study area; C: schematic representation of the study area. The dashed blue line (Ts'04) marks the landward inundation limit of the 2004 Sumatra-Andaman tsunami, as derived from eyewitnesses. D: Aerial view of the study area, highlighting the fish-ponds. E: Close-up view of two ponds and ridges. In the red circle is visible one the pit dug during the field work. Location and elevation data were determined with Leica TS-02 total station and were referenced to high tide shoreline (hts) on site.

## Section S2. Radiocarbon dating

AMS  $^{14}\text{C}$  dating was performed on samples derived from human bones, mollusk shells (terrestrial and marine), charcoal and pottery fragments at the Poznań Radiocarbon Laboratory (Table S1). The samples were collected along two sections oriented NW-SE (Figs. S1, S2). Radiocarbon calibration was obtained with Calib 7.1 by using IntCal 13 for terrestrial samples and Marine 13, with Delta R and R err derived from Southon et al. (2002), for marine samples. All the ages are reported as Calendar years Before Present (Cal yr BP) with a  $2\sigma$  error.

Table S1. Radiocarbon dates, presented as calibrated and uncalibrated ages, with information on the dated material and its significance for the tsunami event chronology. Radiocarbon dating was performed at the Poznan Radiocarbon Laboratory. Radiocarbon calibration was obtained using Calib 7.1 by using IntCal 13 for terrestrial samples and Marine 13, with Delta R and Delta R err derived from Southon et al. (2002), for marine samples.

14C samples list															
Log Name	Depth (cm)	Facies	Material	Specimen	Sample Type	Uncorrected AMS 14C age (yr)	Error (yr)	Calibration curve	Delta R (yr)	Delta R Err (yr)	Calibrated AMS 14C age (yr) 2sigma lower	Calibrated AMS 14C age (yr) 2sigma upper	Significance for tsunami event chronology	Notes	
P4E1	75	Mangrove plain deposit	bone	human	Terrestrial	295	30	IntCal 13			348	459	post-date	↓	2
P4E1	35	Tsunami deposit	shell	<i>Limicolaria</i> sp.	Terrestrial	985	30	IntCal 13			896	959	event age	~	3 (*)
P4E1	35	Tsunami deposit	shell	<i>Limicolaria</i> sp., juvenile	Terrestrial	1025	30	IntCal 13			906	984	event age	~	3 (*)
P3W2	55	Mangrove plain deposit	charcoal		Terrestrial	970	30	IntCal 13			891	933	post-date	↓	2
P3W2	45	Tsunami deposit	shell	<i>Isognomon nucleus</i>	Marine	1890	30	Marine 13	150	40	1197	1385	reworked material		5
P3W2	45	Tsunami deposit	shell	<i>Anadara</i> sp.,	Marine	1455	30	Marine 13	150	40	734	941	event age	~	4
P3W2	15	Alluvial deposit	shell	<i>Achatina</i> sp.	Terrestrial	1315	30	IntCal 13			1226	1295	pre-date	↑	1 (*)
P1E2	28	Tsunami deposit	pottery		Terrestrial	1030	40	IntCal 13			902	1009	event age	~	4
P1E2	28	Tsunami deposit	bone	human	Terrestrial	1010	30	IntCal 13			902	975	event age	=	3
P2E1	63	Tsunami deposit	charcoal		Terrestrial	1000	30	IntCal 13			899	967	event age	~	4
P2E1	60	Tsunami deposit	pottery			none									
P2E1	60	Tsunami deposit	shell	<i>Anadara</i> sp.,	Marine	1470	30	Marine 13	150	40	746	957	event age	~	4
P2E1	45	Alluvial deposit	shell	<i>Achatina</i> sp.	Terrestrial	1450	30	IntCal 13			1299	1389	pre-date	↑	1 (*)
P1S1	45	Mangrove plain deposit	charcoal		Terrestrial	675	30	IntCal 13			632	678	post-date	↓	2 )
P1S1	30	Tsunami deposit	shell	<i>Monetaria annulus</i>	Marine	1415	30	Marine 13	150	40	703	911	event age	~	4
P2E2	47	Tsunami deposit	shell	<i>Melampus semiauratus</i>	Terrestrial	1560	30	IntCal 13			1387	1529	reworked material		5 (*)
P2E2	40	Alluvial deposit	charcoal		Terrestrial	970	30	IntCal 13			891	933	pre-date	↑	1
K1	23	Tsunami deposit	charcoal		Terrestrial	1025	30	IntCal 13			906	984	event age	=	3
K1	18	Tsunami deposit	bone	human	Terrestrial	963	28	IntCal 13			891	930	event age	=	3
			↑ pre-date tsunami event				↓ post-date tsunami event				~ age may be older or younger than the tsunami event			= most reliable tsunami event age	



pre-date tsunami event



post-date tsunami event



age may be older or younger than the tsunami event



most reliable tsunami event age

Notes:

- 1- The samples collected within alluvial plain deposits pre-date the interpreted tsunami event. The samples consist of terrestrial mollusks, exception for P2E2cm40, which is charcoal. In alluvial environments, sediments and the associated material used for radiocarbon dating may be transported and re-deposited during river floods, and consequently the radiocarbon ages may provide older ages with respect to the hosting sediment.
  - 2- The samples collected within the mangrove plain deposits, consisting of human bones and charcoal, post-date the tsunami event. All the samples analysed are assumed to be in place and diagnostic of the age of the sediments.
  - 3- The samples collected within the tsunami deposit and consisting of charcoal, pottery, and human bones best represent the age of the tsunami event. Charcoal was probably originated from the fire pits used by the Swahili inhabitants for domestic purposes and was then transported by the tsunami waves.
  - 4- Large marine and terrestrial mollusks collected in the tsunami deposit may potentially have slightly older ages with respect to the tsunami event, as they may have been harvested for food or ornamental purposes prior to the tsunami.
  - 5- Two samples, a terrestrial and a marine shell, collected in the tsunami deposit have older ages respect to the age of the tsunami event inferred from samples of types 3 and 4. We interpret these two samples as reworked material, eroded by the tsunami wave from older sediments and transported inland. This interpretation is supported by the fact that the two samples have similar, or older, ages respect to the samples extracted from the alluvial deposit that pre-date the tsunami event.
- (\*) Terrestrial snails may incorporate carbon from ancient sources as a result of their dietary behaviour thus providing older radiocarbon ages (Hill et al., 2017).



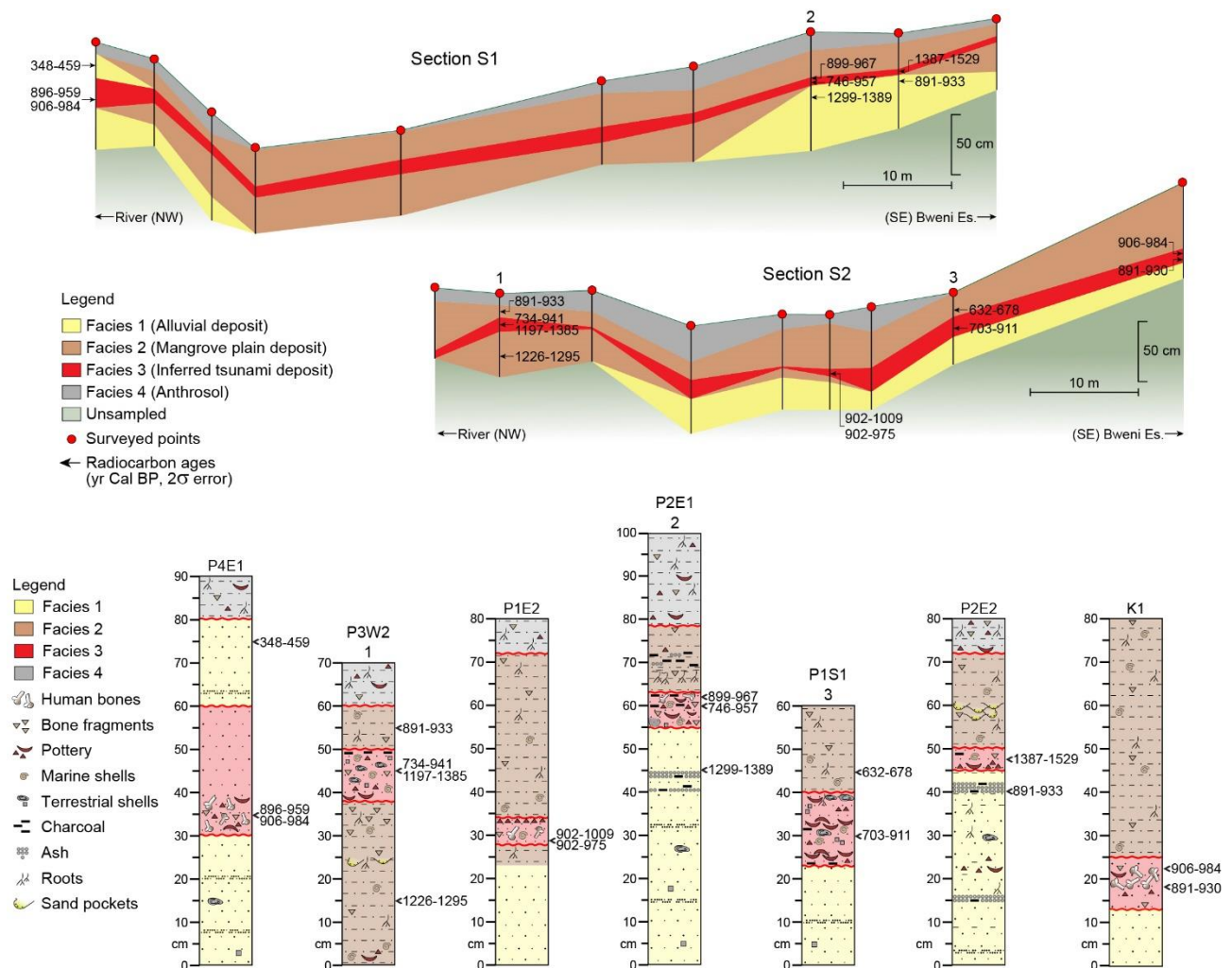


Figure S2. Sampled sections for radiocarbon dating. Ages are reported in Calendar years BP.

### Section S3. Sediment grain size

Grain size analyses were performed using a Malvern<sup>TM</sup> Mastersizer 2000 laser diffraction particle size analyser equipped with a Hydro 2000MU manual inlet system. Samples were first treated with 30% H<sub>2</sub>O<sub>2</sub> to remove organic matter and then dispersed in sodium hexametaphosphate. The Malvern<sup>TM</sup> Mastersizer 2000 measures the volume scattering function in 100 bins based on Mie scattering theory and reports the grain size spectra in volume percent (as opposed to particle number or mass) per bin as a function of grain size or phi. Measurement parameters assume the grains are irregularly-shaped, opaque particles with an index of refraction equal to quartz. Distilled water is used as the dispersant. During measurement, grains from each sample were kept in suspension using a pumping speed of 2500 rpm. Each sample was measured in triplicate following 1 minute of sonication to disperse particles.

The tsunami deposit lacks a landward-fining trend, and this is likely due to the mixing of different sediment populations within the deposit itself, as noted in previously documented tsunami layers

(Moore et al., 2006; Moore et al., 2007a). Because each sediment sample represents a mixture of particles delivered by multiple processes or from differing sources that vary spatially and temporally, the grain size spectra were unmixed to determine the number of populations present in the data set using sample-based, varimax-rotated, principal component analysis (VPCA; following Woodward, 2007; Darby et al., 2009; Ortiz, 2011; Fig. S3). This method has previously been successfully applied to tsunami deposits to tease apart end member contributions from different populations of grains present in mixed samples (Woodward, 2007). The VPCA method is an eigenvalue-eigenvector decomposition that can be used to partition the correlation matrix from complex data sets into independent end members. Indeed, the VPCA of the sediment grain-size demonstrates that the tsunami deposit results from two sediment sources: one finer and generally better sorted consistent with the alluvial plain deposit (1st component, 60.49% information), and one coarser and more poorly sorted consistent with the mangrove plain deposit (2nd component, 36.39% information). We suggest that a landward-directed surge of water mobilised sediment from the beach, mixed it with sediment eroded from the terrestrial land surface, and deposited that mixture inland. In such a scenario, coastal sand would dominate the seaward portion of the deposit, while terrestrial sediment would become more prominent inland (see supplementary material). Overall grain size within the deposit would remain constant or coarsen landwards controlled by the sediment source ratio, rather than distance from the source. In any event sorting of the sediment would become worse inland due to progressive mixing of the two sediment sources. Additionally, the Bweni Escarpment limited the inland propagation of the wave, also masking a landward grain-size fining trend.

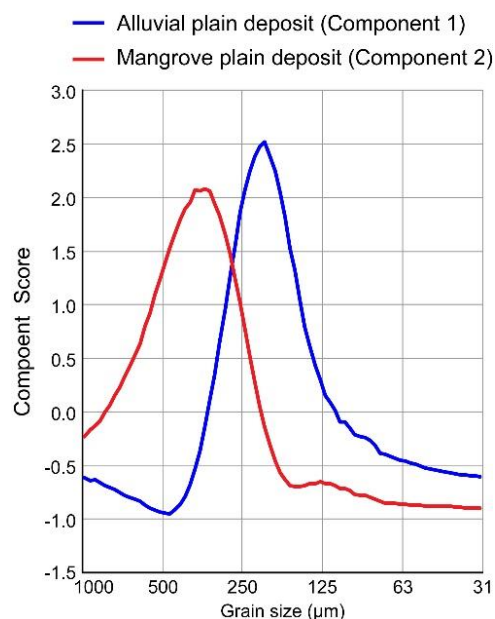


Figure S3. Dimensionless grain size component scores as a function of  $\mu\text{m}$  for the coarser (Alluvial deposit, blue curve) and the finer (Mangrove plain deposit, red curve) components extracted from the grain size spectra of the tsunami deposit using sample-based, varimax-rotated, principal component analysis.

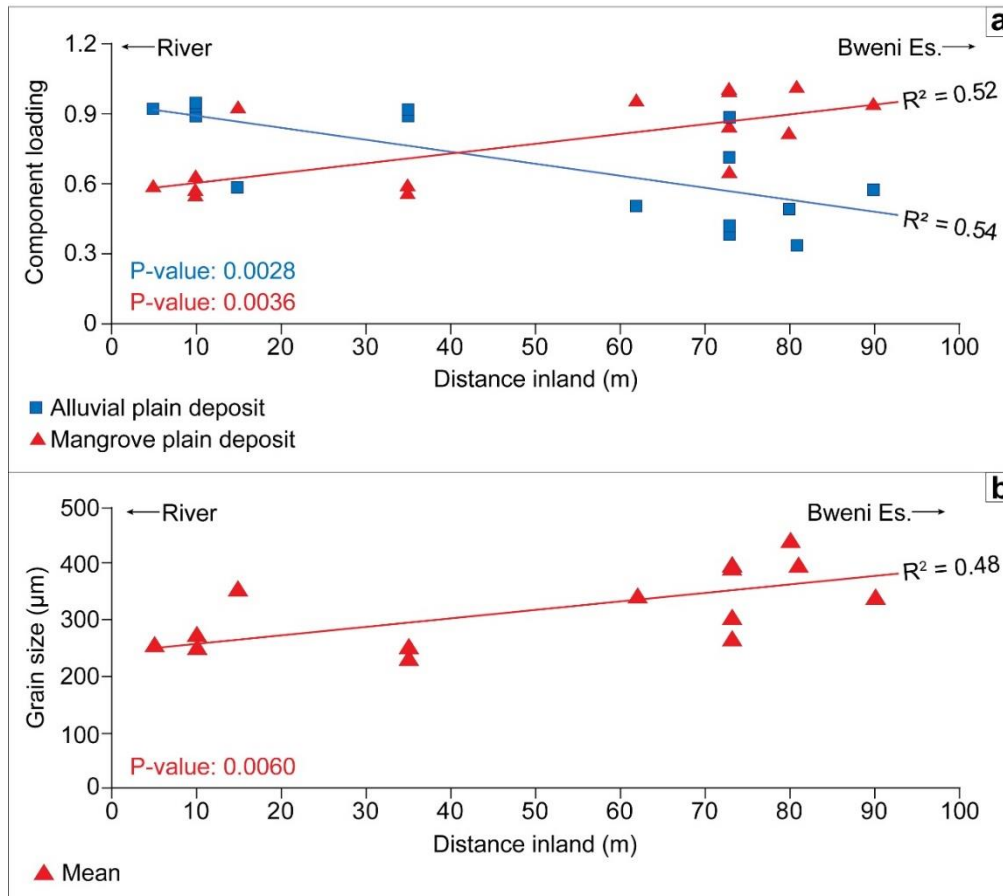


Figure S4. a) Results of sample-based, varimax-rotated, principal component analysis on the tsunami deposit, showing relative proportion of alluvial deposit (component 1) and mangrove plain deposits (component 2) in each location. b) Change in mean grain size of the tsunami deposit with distance inland.

#### Section S4. Paleoenviromental reconstructions

Micro- and macro-paleontological analyses were obtained on samples collected from the sediment exposed in the pits and trenches, at variable intervals depending on the lithology (Fig. S1). Location and elevation of each stratigraphic column (referred to mean high water) were determined with a Leica TS-02 total station and a GPS. The samples were oven dried at 50 °C, washed through a 63  $\mu\text{m}$  sieve and dried again. The fraction  $>63 \mu\text{m}$  was examined under the optical stereomicroscope for semiquantitative analyses. Reconstruction of depositional environments were based upon the integration of fossil remains including mollusks, foraminifera, fish, insects, and small vertebrates, all valuable ecological indicators (Figs. S5, S6). Marine and transitional (estuarine, mangals) macrofauna includes bivalves *Anadara*, *Saccostrea*, *Isognomon*, and gastropods *Monetaria*, *Polinices*, *Phosinella*, *Cerithidea*, *Melanoides*, *Melampus*. In addition, the layer contains land snails (subulinids, *Achatina*, *Limicolaria*). The microfauna is mainly shallow marine benthic foraminifera such as *Nonion*, *Elphidium* and *Ammonia*.

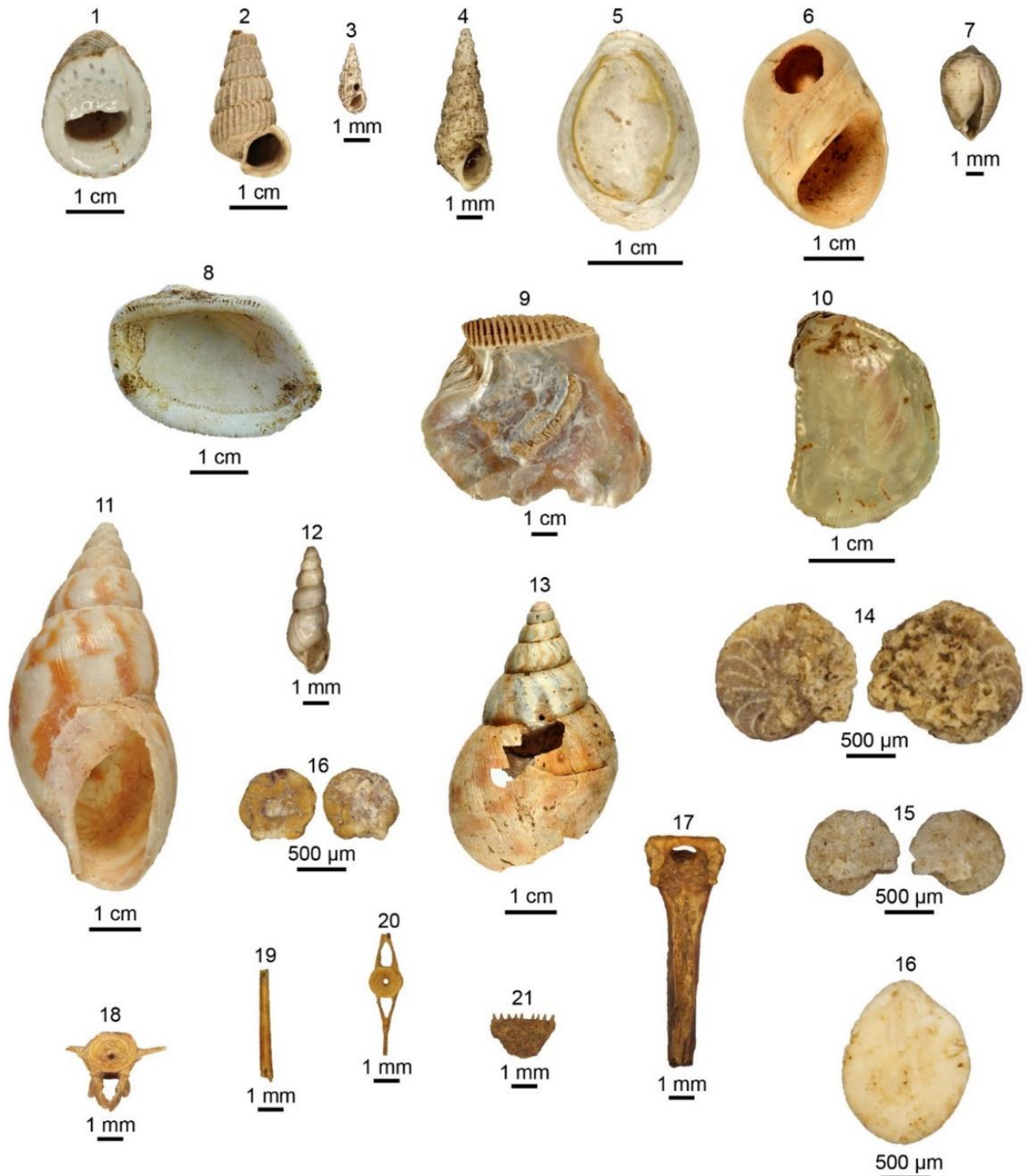


Figure S5. Macro and micro faunas sampled within the tsunami deposit. 1 *Nerita albicilla* (Linnaeus, 1758); 2 *Cerithidea decollata* (Linnaeus, 1767); 3 *Phosinella* cf. *phormis* (Melvill, 1904); 4 *Melanoides tuberculata* (O. F. Müller, 1774); 5 *Monetaria annulus* (Linnaeus, 1758); 6 *Polinices mammilla* (Linnaeus, 1758); 7 *Melampus semiauratus* (Connolly, 1912); 8 *Anadara* sp.; 9 *Isognomon nucleus* (Lamarck, 1819); 10 *Saccostrea cucullata* (Born, 1778); 11 *Limicolaria* sp.; 12 Subulinidae sp.; 13 *Achatina* sp.; 14 *Nonion* sp., 15 *Elphidium* sp., *Ammonia* sp., 16 Miliolide sp., 17 Bone (undetected, probably small mammal); 18-21 Fish bones.

The inferred tsunami deposit shows laterally variable sedimentary facies and it hosts human bones and archeological remains belonging to a Swahili maritime community (Fig. S6).



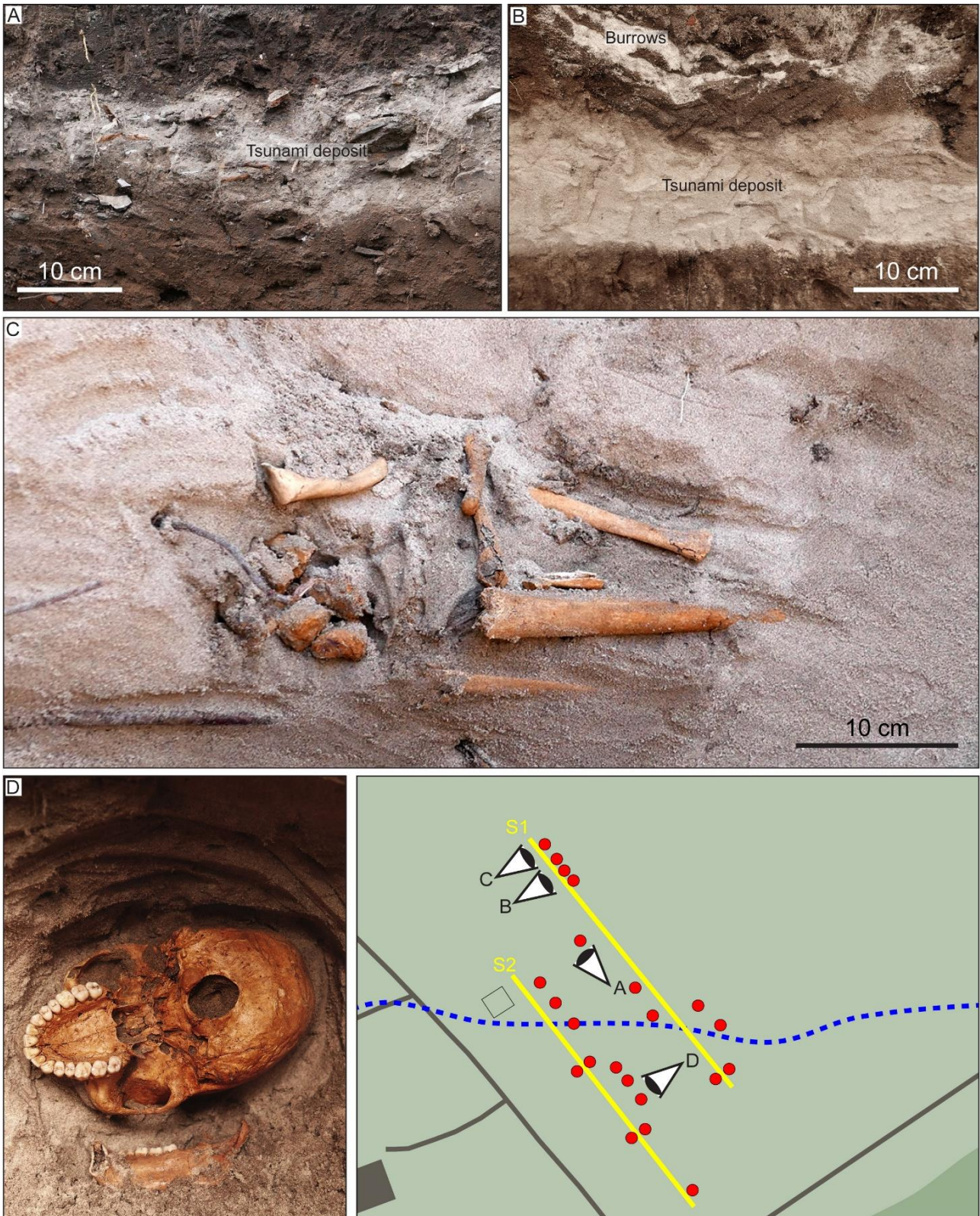


Figure S6. Sedimentary facies of the tsunami deposit at different locations, containing archeological remains (A) and human bones (C and D).

## Section S5. Tsunami Simulation

To simulate the tsunami inundation in Pangani Bay (Tanzania) we used the COMCOT tsunami numerical model (Liu, 1998; Wang and Power, 2011). The numerical model can solve the linear and

non-linear shallow water equations in Spherical coordinates. In deep ocean basins, the tsunami wave amplitude is usually much smaller than the water depth and linear shallow water equations may be applied to describe the tsunami evolution. The wavelength becomes shorter and the amplitude larger due the shallowness of water as the tsunami propagates onto a continental shelf towards coastal areas. As a result, the linear shallow water equations gradually become invalid and nonlinear effects will dominate. The nonlinear shallow water equations including bottom friction effects and need to be used to describe the wave motion in the coastal zone and inundation process (Liu et al., 1995). Using a nested grid system, different spatial resolutions may be used for the different stages of tsunami evolution, which allows us to study the entire life-span of a tsunami simultaneously, from its generation in the source area to inundation in coastal regions. We used a nested grid system with grid sizes of 30, 15, 5, 1, 0.5, 0.1 arc-sec. The Manning's roughness coefficient that is assumed in the simulation is 0.025, a value widely used in tsunami inundation modelling (Imamura, 2009). The GEBCO global bathymetry data was used for low resolution tsunami simulation. For the high-resolution simulation in Pangani, the topography of the coastline is derived using an aerial photogrammetric technique with data acquired through an unmanned aerial vehicle, while the bathymetry (1-m-spaced isobaths) is derived from a navigation map.

#### *SM5.1. Earthquake Fault Model*

We simulated the tsunami inundation in Pangani using scenarios based on the 2004 earthquake, 1833 earthquake and Makran Subduction Zone earthquake. For the 2004 Sumatra-Andaman earthquake, the source model estimated from satellite altimetry data (Hirata et al., 2006) is used in the simulation. The total length of the fault model is 1300 km, each sub-fault is 100 km long and 150 km wide. The maximum slip amount is 29 m and the total seismic moment calculated from the slip distribution is  $9.86 \times 10^{22}$  Nm (Mw 9.3).

Studies of co-seismic uplifts based on the stratigraphy of coral microatolls in Mentawai Island, off the west coast of Sumatra Indonesia suggest that the region experienced a great tsunamigenic earthquake in 1833 (Natawidjaja et al., 2006). This event was used as a basis for a hypothetical earthquake source model with length of 900 km, width of 175 km, strike of  $322^\circ$ , dip of  $12^\circ$ , rake of  $90^\circ$  and slip amount 15 m (Okal and Synolakis, 2008). This fault model has a seismic moment of  $9.45 \times 10^{22}$  Nm (Mw 9.3), which is similar to that of the 2004 earthquake.

Another possible earthquake source for a tsunami in Pangani is in Makran Subduction Zone. According to Okal and Synolakis (2008) at least four large tsunamigenic earthquakes occurred in this subduction zones in 1851, 1864, 1945, and 1765. The paper also suggests an extreme worst-case tsunamigenic earthquake scenario in the region with a total fault length of 900 km, width of 100 km,

dip of  $7^\circ$ , rake of  $90^\circ$ , and slip amount of 15 m. This fault model has a seismic moment of  $5.40 \times 10^{22}$  Nm (Mw 9.1). We used this fault model to simulate the tsunami in Pangani.

For all the three earthquakes, we simulated the tsunami in Pangani at both low tide and high tide (Fig. S7). A 30-days tidal data at a station in Zanzibar, Tanzania (<https://www.psmsl.org>) near Pangani, shows that the maximum tidal range is 4.5 m, suggesting the highest high tide is approximately 2 m from the mean sea level. In the tsunami simulation, we used the tidal range of 2 m as a water level offset in the initial condition.

Tide gauge data are not available for the Zanzibar station during December 2004. The nearest data to Pangani are from the Lamu gauging station (Kenya), reported in Figure S7.

### **Section S6. Eyewitnesses of the 2004 tsunami in Pangani**

The tsunami arrival in East Africa was recorded during a low tide of a spring tidal cycle (Fig. S7). Local eyewitnesses to the 2004 tsunami estimated the inundation distance and flow depth of the waves at the site of this study. They described the tsunami as an anomalous train of three main waves that flooded the study area at about 1-hour intervals during a low tide. The water level raised about 1 meter above the high tide shoreline (Fig. S1), leaving a few-cm-thick layer of mud after its retreat. Some 15 years since the 2004 tsunami, no signs of this event were discovered in the investigated sedimentary record. A limited preservation potential of the 2004 tsunami deposit has been documented in Sri Lanka (Moore et al., 2007b) and Thailand (Szczuinski, 2012), much closer to the Sunda Trench than the study area, due to the erosion generated by Monsoon rains.



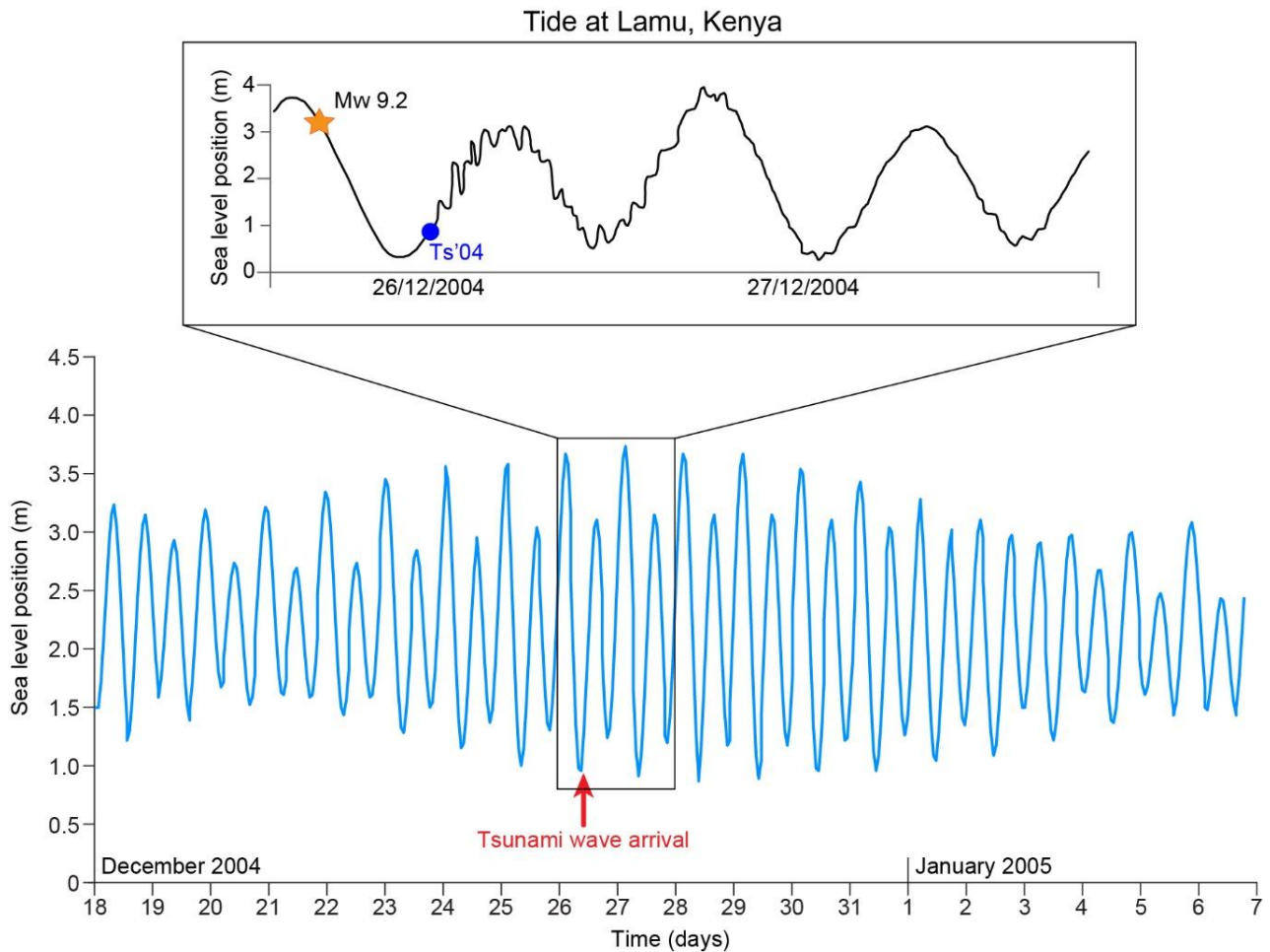


Figure S7. Tidal amplitude recorded at the Lamu gauging station (Kenya). Data from: <https://uhslc.soest.hawaii.edu/>. The red arrow marks the timing of the first tsunami wave arrival in Tanzania. The tsunami arrival at Lamu was recorded during spring low tide.

## Section S7. Ethics statement

The field site on the southern flank of the Pangani Bay was discovered by Dr. Mjema (Department of Archeology, University of Dar es Salaam), who invited the team to visit the study area. All the personnel involved in the project had the official authorization to perform field activities by the University of Dar es Salaam, Department of Archeology and Department of Geology, and the local administration in the town of Pangani, who observed the work in the field. The study was carried out on land belonging to the Institute of Marine Sciences of the University of Dar es Salaam, which supervised the field activities, provided permission to conduct geological surveys and to collect sediment samples. The sedimentological data presented in this study were collected during the summer of 2017. The archaeological remains encountered during the field activities were viewed with respect, treated with care, and left in place following archeological procedures and the guidelines provided by the National Geographic Society and the Society for Historical Archeology. Five fragments of a few grams of organic material were carefully extracted from the sand layer without compromising the archeological site and used for performing radiocarbon dating (see Table S1). The



export of sediment samples for analyses was approved by the United Republic of Tanzania with an export permit for minerals and samples of minerals. No endangered or protected species were affected during the field activities.

## Reference

- Darby, D.A., Ortiz, J., Polyak, L., Lund, S., Jakobsson, M., and Woodgate, R.A., 2009, The role of currents and sea ice in both slowly deposited central Arctic and rapidly deposited Chukchi–Alaskan margin sediments: *Global and Planetary Change*, v. 68, p. 58–72.
- Hill, E.A., Reimer, P.J., Hunt, C.O., Prendergast, A.L., and Barker, G.W., 2017, Ecology of the land snail *Helix Melanostoma* in Northeastern Libya; *Radiocarbon*, v. 59, p. 1521–1542.
- Hirata, K., Satake, K., Tanioka, Y., Kuragano, T., Hasegawa, Y., Hayashi, Y., and Hamada, N., 2006, The 2004 Indian Ocean tsunami: Tsunami source model from satellite altimetry: *Earth, planets and space*, v. 58, p. 195–201.
- Imamura, F., Bernard, E.N., and Robinson, A., 2009, Tsunami modeling: calculating inundation and hazard maps: *The sea*, v. 15, p. 321–332.
- Liu, P.L.F., Cho, Y.S., Yoon, S.B., and Seo, S.N., 1995, Numerical simulations of the 1960 Chilean tsunami propagation and inundation at Hilo, Hawaii, *in* *Tsunami: Progress in prediction, disaster prevention and warning* (pp. 99-115). Springer, Dordrecht.
- Liu, P.L.F., Woo, S.B., and Cho, Y.S., 1998, Computer programs for tsunami propagation and inundation. Cornell University, p. 25.
- Moore, A.L., Nishimura, Y., Gelfenbaum, G., and Kamataki, T., 2006, Sedimentary deposits of the 26 December 2004 tsunami on the northwest coast of Aceh, Indonesia: *Earth, Planets, and Space*, v. 58, p. 53–258.
- Moore, A.L., McAdoo, B., and Ruffman, A., 2007, Landward fining from multiple sources in a sand sheet deposited by the 1929 Grand Banks tsunami, Newfoundland: *Sedimentary Geology*, v. 200, p. 336–346.
- Moore, A.Al., McAdoo, B.G., and Ranasinghe, N., 2007b, 2004 South Asia tsunami left little record of its trace near Yala, southeastern Sri Lanka: AGU Fall Meeting Abstracts.
- Natawidjaja, D., Sieh, K., Chlieh, M., Galetzka, J., Suwargadi, B., Cheng, H., Edwards, R.L., Avouac, J.P., and Ward, S., 2006, Source parameters of the great Sumatran megathrust earthquakes of 1797 and 1833 inferred from coral microatolls: *Journal of Geophysical Research*, v. 111, B06403.
- Okal, E.A., and Synolakis, C.E., 2008, Far-field tsunami hazard from mega-thrust earthquakes in the Indian Ocean: *Geophysical Journal International*, v. 172, p. 995–1015.
- Ortiz, J.D., 2011, Application of visible/near infrared derivative spectroscopy to Arctic paleoceanography: IOP Conf. Series: Earth and Environmental Science, v. 14, doi:10.1088/1755-1315/14/1/012011.
- Southon, J., Kashgarian, M., Fontugne, M., Metivier, B., and Yim, W.W-S., 2002, Marine reservoir corrections for the Indian Ocean and Southeast Asia: *Radiocarbon*, v. 44, p. 167–180.
- Szczuciński, W., 2012, The post-depositional changes of the onshore 2004 tsunami deposits on the Andaman Sea coast of Thailand: *Natural Hazards*, v. 60, p. 115–133.
- Wang, X., and Power, W.L., 2011, COMCOT: a tsunami generation propagation and run-up model: GNS Science.
- Woodward, S., 2009, Principle Component Analysis of Sediment Deposited in the Village of Titiana from the Solomon Islands Tsunami of April 2, 2007. Kent State University, Department of Geology, MS Thesis, Kent, OH, 55p.